Monthly Notices
of the
ROYAL ASTRONOMICAL SOCIETY

Mon. Not. R. Astron. Soc. **415,** 3033–3041 (2011) doi:10.1111/j.1365-2966.2011.18927.x

Limiting eccentricity of subparsec massive black hole binaries surrounded by self-gravitating gas discs

C. Roedig,[1⋆] M. Dotti,[2,3] A. Sesana,[1] J. Cuadra[2,4] and M. Colpi[3]

[1]*Max-Planck-Institut für Gravitationsphysik, Albert Einstein Institut, Am Mühlenberg 1, D-14476 Golm, Germany*
[2]*Max-Planck-Institut für Astrophysik, Karl-Schwarzschild-Str. 1, D-85748 Garching, Germany*
[3]*Università di Milano Bicocca, Dipartimento di Fisica G. Occhialini, Piazza della Scienza 3, I-20126 Milano, Italy*
[4]*Departamento de Astronomía y Astrofísica, Pontificia Universidad Católica de Chile, Vicuña Mackenna 4860, 7820436 Macul, Santiago, Chile*

Accepted 2011 April 18. Received 2011 April 15; in original form 2011 February 25

ABSTRACT

We study the dynamics of supermassive black hole binaries embedded in circumbinary gaseous discs, with the smoothed particle hydrodynamics code GADGET-2. The subparsec binary (of total mass M and mass ratio $q = 1/3$) has excavated a gap and transfers its angular momentum to the self-gravitating disc ($M_{\rm disc} = 0.2M$). We explore the changes of the binary eccentricity, e, by simulating a sequence of binary models that differ in the initial eccentricity e_0 only. In initially low-eccentric binaries, the eccentricity increases with time, while in high-eccentric binaries e declines, indicating the existence of a limiting eccentricity $e_{\rm crit}$ that is found to fall in the interval [0.6, 0.8]. We also present an analytical interpretation for this saturation limit. An important consequence of the existence of $e_{\rm crit}$ is the detectability of a significant residual eccentricity $e_{\rm LISA}$ by the proposed gravitational wave detector *Laser Interferometer Space Antenna (LISA)*. It is found that at the moment of entering the *LISA* frequency domain $e_{\rm LISA} \sim 10^{-3}$–$10^{-2}$, a signature of its earlier coupling with the massive circumbinary disc. We also observe large periodic inflows across the gap, occurring on the binary and disc dynamical time-scales rather than on the viscous time. These periodic changes in the accretion rate (with amplitudes up to ∼100 per cent, depending on the binary eccentricity) can be considered a fingerprint of eccentric subparsec binaries migrating inside a circumbinary disc.

Key words: accretion, accretion discs – black hole physics – gravitational waves – methods: numerical.

1 INTRODUCTION

Supermassive black hole (BH) binaries are currently postulated to form in the aftermath of galaxy mergers (Begelman, Blandford & Rees 1980), despite the difficulties, still present, in identifying them observationally (see Colpi & Dotti 2009 for a review). Thanks to advances in N-body/hydrodynamical simulations, it has been shown that major mergers of gas-rich disc galaxies with central BHs are conducive to the formation of eccentric BH binaries (e.g. Mayer et al. 2007). Orbiting inside the massive gaseous nuclear disc resulting upon collision, the two BHs continue to lose orbital energy and angular momentum under the large-scale action of gas-dynamical friction, and end up forming a circular Keplerian binary, on parsec scales (Escala et al. 2005; Dotti et al. 2007, 2009). As the gaseous and stellar mass content inside the BH orbit continues to decrease in response to the hardening of the binary, further inspiral is believed to be controlled by the action of either three-body scattering of individual stars and/or the interaction of the binary with a circumbinary gaseous disc (e.g. Armitage & Natarajan 2002; Merritt & Milosavljević 2005).

The gravitational interaction of the massive BH binary with the gaseous disc is believed to be of foremost importance to assess not only its observability on subparsec scale, but also its fate. Gravitational waves (GWs) start to dominate the BH inspiral (leading to coalescence) only at tiny binary separations, of the order of a few milliparsec for a binary of $M \approx 10^6\,{\rm M}_\odot$. If a viscous disc is present, Lindblad resonances can cause BH migration down to the GW inspiral domain (e.g. Papaloizou & Pringle 1977; Goldreich & Tremaine 1980). Following this proposal, a number of studies have modelled BH migration in Keplerian, geometrically thin α-discs (Ivanov, Papaloizou & Polnarev 1999; Gould & Rix 2000; Armitage & Natarajan 2002; Haiman, Kocsis & Menou 2009; Lodato et al. 2009).

Using high-resolution hydrodynamical simulations, Cuadra et al. (2009) recently investigated the evolution of the orbital elements of a massive BH binary, under the hypotheses that (i) the binary, at the radii of greatest interest (tenths of a parsec), is surrounded

⋆E-mail: croedig@aei.mpg.de

by a self-gravitating, marginally stable disc and (ii) the binary has excavated in its surroundings a cavity, i.e. a hollow density region of a size nearly twice the binary orbital separation, due to the prompt action of the binary's tidal torques. The simulations highlight one key aspect: that of the *increase* of the binary *eccentricity*, e, during the decay of its semimajor axis. The excitation of e was already noted and studied in Armitage & Natarajan (2005), who investigated BH orbital decay in the presence of a Keplerian α-disc in two dimensions, as well as in earlier analytical work by Goldreich & Sari (2003) in the context of type II planet migration.

The increase of e has a number of interesting consequences. First, for a given semimajor axis, binaries with larger e will lose energy substantially faster via GWs, coalescing on a shorter time-scale (Peters & Mathews 1963). Secondly, accretion streams that leak through the cavity and fuel the BHs happen with a better defined periodicity in the case of eccentric binary (e.g. Artymowicz & Lubow 1996), likely increasing the chance of BH binary identification through active galactic nucleus time-variable activity. Finally, more eccentric binaries will retain some residual eccentricity when detectable by the *Laser Interferometer Space Antenna* (*LISA*; Berentzen et al. 2009; Amaro-Seoane et al. 2010; Sesana 2010). For these reasons it is important to understand if, under disc-driven migration, the eccentricity keeps on growing up to $e \approx 1$ or if there is a limiting eccentricity towards which the binary orbit tends.

In this paper, we explore the binary–disc interaction with high-resolution N-body hydro simulations, modelling the circumbinary disc as in Cuadra et al. (2009) (see Section 2). However, instead of starting with binaries with low eccentricities, we now construct a sequence of binaries with fixed semimajor axis, BH and disc–BH mass ratios but with different initial eccentricities e_0, varying it from 0.2 to 0.8. The binaries interact with a self-gravitating disc changing their orbital elements. With this approach we assess whether the eccentricity growth saturates, and at which value. We present a simple analytical interpretation of our numerical results in Section 4. If the saturation eccentricity is large, then the binary may reach coalescence with some residual eccentricity, after GW emission has reduced it considerably. This issue was already discussed in Armitage & Natarajan (2005) as a possible discriminant between gas-driven versus stellar-driven inspiral. In Section 5 we revisit this question in detail, in the context of the proposed *LISA* mission. The simulations also provide information on gas streams that leak through the cavity. We investigate how the variability properties of the accretion rate on to the BHs depend on the binary eccentricity. This analysis may lead to the identification of BH close binaries and estimates of their orbital elements (Section 5).

2 SIMULATION SET-UP

2.1 The model

We model a system composed of a binary BH surrounded by a gaseous disc. Since we are interested in the subparsec separation regime, we assume that the binary torque has already excavated an inner cavity in the gas distribution. We also assume that the cooling rate is long relative to the dynamical time-scale, preventing disc fragmentation (e.g. Rice, Lodato & Armitage 2005). We consider a binary with an initial mass ratio[1] $q = M_2/M_1 = 1/3$ and a disc with an initial mass $M_{\rm disc} = 0.2M$, where $M = M_1 + M_2$ is the total mass of the binary. The binary has initial eccentricity e_0, semimajor axis a_0 and initial dynamical time $t_{\rm dyn} = f_0^{-1} = 2\pi/\Omega_0$, where $\Omega_0 = (GM/a_0^3)^{1/2}$. Both the binary and the disc rotate in the same plane and direction as expected from the simulations of Dotti et al. (2009). The disc is initially axisymmetric, and extends from $2a_0$ to $5a_0$. Its initial surface density profile is given by $\Sigma(R) \propto R^{-1}$, where R is the distance to the centre of mass (COM) of the system.

[1] Unless otherwise stated, subscripts 1 and 2 refer to the primary (more massive) and secondary (less massive) BH, respectively.

2.2 Early evolution

Cuadra et al. (2009) modelled the evolution of low-eccentricity binaries in the system discussed above. They found that self-gravity drives the initially uniformly distributed gas into a ring-like configuration located at $R \approx 3a_0$. This ring eventually collapses and later spreads again in roughly the same radial range it had in the initial conditions ($2a_0$–$5a_0$). However, instead of having a uniform density distribution, the disc displays a clear spiral pattern. Cuadra et al. (2009) found that this configuration remains stable for at least $3000\,\Omega_0^{-1}$, and that during this time the binary both shrinks and gains eccentricity due to its interaction with the disc. In this study, we skip the early transient evolution and start from a snapshot taken at $t = 500\,\Omega_0^{-1}$. At this time, the disc has already settled into the steady-state configuration.

2.3 The new simulations

Our goal is to study the secular evolution of the binary–disc system, focusing in the evolution of the binary eccentricity. The ideal method would be to follow the binary from an initial, parsec-scale separation, until it reaches the GW-dominated regime. Unfortunately such an approach is not feasible. The time-scale for decay is $\sim 10^4\,\Omega_0^{-1}$ (Cuadra et al. 2009), much longer than what we can feasibly simulate with current computational power. Moreover, as the binary shrinks, its angular momentum is transferred to the disc. Without appropriate boundary conditions, this results in the unphysical expansion of the disc, slowing further the evolution of the system (Cuadra et al. 2009). To accomplish our goal we take an indirect approach. We run a set of simulations where the gas configuration was taken from the steady state of a previous simulation, as described above, but the binary had different initial eccentricities. The energy of the binary was conserved, i.e. its semimajor axis a was fixed, only the angular momentum of the binary was changed to accomplish the various initial eccentricities e_0. We then extrapolate the long-term evolution of the eccentricity interpreting the results of the different runs as snapshots of the binary life taken at different ages.

2.4 Numerical method

To simulate the binary–disc system, we use the numerical method described in detail by Cuadra et al. (2009). We use a modified version of the smoothed particle hydrodynamics (SPH) code GADGET-2 (Springel 2005). We allow the gas to cool on a time-scale which is proportional to the local dynamical time of the disc. To prevent it from fragmenting, we set $\beta = t_{\rm cool}/t_{\rm dyn} = 10$. Unlike Cuadra et al. (2009), we assume that the small amount of gas present in the inner cavity ($r \lesssim 1.75a$) is isothermal, with an internal energy per unit mass $u \approx 0.14(GM/R)$. The effect of this recipe is to confine the gas in the inner region to a relatively thin geometry. The gravitational interaction between particles is calculated with a Barnes–Hut tree. For all runs we use two million particles, a number which has been

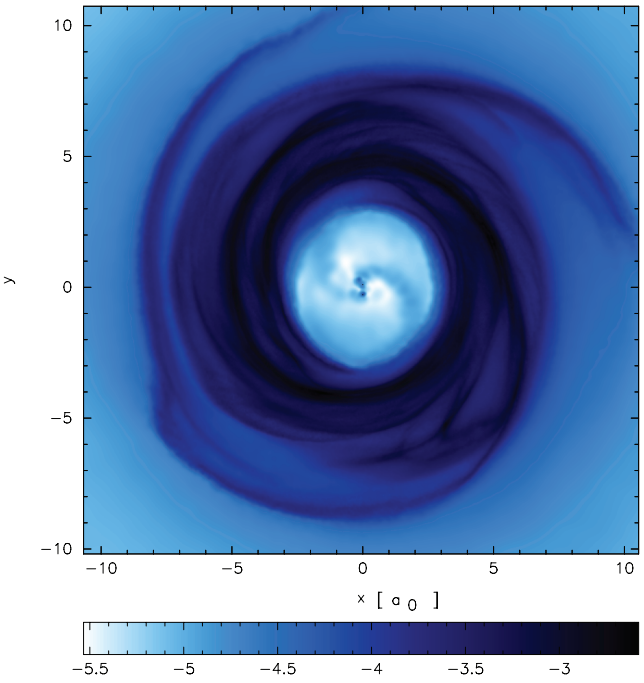

Figure 1. Face-on view of the circumbinary disc surrounding a BH binary of initial eccentricity $e_0 = 0.6$ after 180 orbits. The gas density is colour-coded on a logarithmic scale with brighter colours corresponding to lower gas density; axes in units of a_0. The figure shows the spiral patterns excited in the disc, the gap surrounding the binary and the yin-yang-shaped gas inflows around the BHs. Figure made using SPLASH (Price 2007).

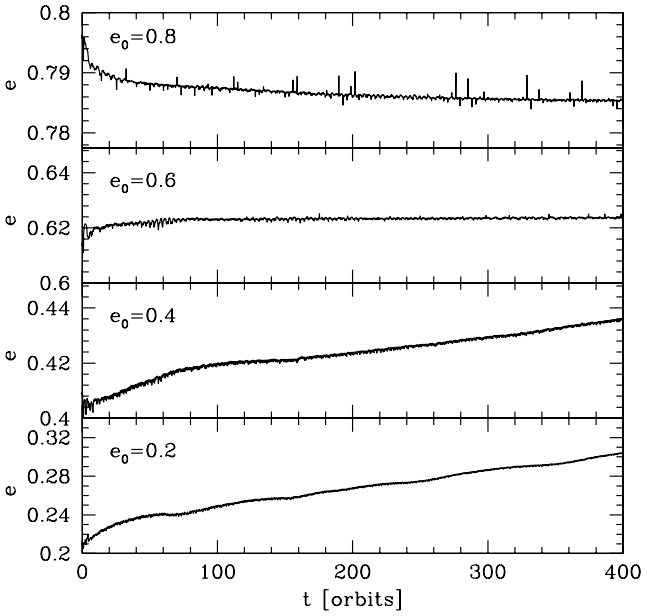

Figure 2. The eccentricity evolution of the four standard runs: $e_0 = 0.2$, 0.4, 0.6, 0.8, starting from bottom to top.

shown to be sufficient by Cuadra et al. (2009). Since we are interested in following the evolution of the binary orbit accurately, we take the BHs out of the tree and compute the gravitational forces acting on them directly, i.e. summing up the contributions from each gas particle. Moreover, to ensure an accurate integration, the dynamics of the BHs is followed with a fixed time-step, equal to $0.01\,\Omega_0^{-1}$. The BH binary is modelled as a pair of point masses, and their potentials are assumed to be Newtonian. Relativistic corrections, important only when the binary separation decays below $\sim$2 Mpc (Peters & Mathews 1963), are not included in the SPH simulations but are considered in Section 5, when estimating the eccentricity of binaries entering the *LISA* band. Gas particles approaching either BH are taken away from the simulation in order to avoid the very small time-steps they would require. They are considered to be accreted, and their mass and momentum are transferred to the corresponding BH (Bate, Bonnell & Price 1995; Cuadra et al. 2006). In the present simulations the sink radius around each BH, below which particles are accreted, is set to $0.03a_0$. A face-on view of the disc surface density is shown in Fig. 1 in which the gas has already relaxed around a binary of $e_0 = 0.6$. It shows the typical spiral arms in the disc and the resonant streams in the inner gap region.

3 ECCENTRICITY EVOLUTION

As described in Section 2.3, we prepared four initial conditions identical but for the initial values of the binary eccentricity. In Fig. 2 we show the evolution of e for four runs with initial eccentricities $e_0 = 0.2$, 0.4, 0.6, 0.8, respectively (bottom to top). The bottom panel depicts the monotonic rise of e, for the run with $e_0 = 0.2$: the eccentricity increases almost linearly after the first $70 f_0^{-1}$. The run for $e_0 = 0.4$ (second panel) displays a similar behaviour, but the slope $\mathrm{d}e/\mathrm{d}t$ is much shallower (note the different scales in the y-axes of Fig. 2). In the third panel, corresponding to $e_0 = 0.6$, we observe a fast increase of the eccentricity up to $e = 0.62$ within the first few orbits; afterwards the eccentricity saturates, approaching a constant with $\mathrm{d}e/\mathrm{d}t \sim 0^+$. The top panel refers to the run with the largest initial eccentricity explored, $e_0 = 0.8$. This time the eccentricity exhibits a negative slope with $\mathrm{d}^2e/\mathrm{d}t^2$ steadily decreasing until $\mathrm{d}e/\mathrm{d}t \sim 0^-$.

The key result, illustrated in Fig. 2, is the existence of a limiting $e_{\rm crit}$ that the BH binary approaches in its interaction with the disc. Since the runs were halted after 400 orbital cycles, we can only bracket the interval in which $e_{\rm crit}$ lies: $e_{\rm crit} \in [0.62, 0.78]$. The reason of this uncertainty is technical as we find that the decline of e is very hard to follow numerically due to the fast expulsion of the gas out of the region where torques can still effectively interact with the BH binary – an effect that increases with the binary eccentricity, as expected. Indeed, if we define $R_{\rm gap}$ as the inner location of the disc's half-maximal surface density, we find that the gas moves from an initial value of $R_{\rm gap} \approx 2a_0$ to a time-averaged value of $\approx 2.6a_0$, $3.0a_0$, $3.4a_0$ and $3.8a_0$ during the first 53 binary orbits, for the runs with an initial binary eccentricity of 0.2, 0.4, 0.6 and 0.8, respectively. Such an expansion of the gas is not unexpected since no outer inflow boundary conditions were implemented in our simulations. While the rate of eccentricity change is affected by the expansion resulting from the initial orbital set-up, its long-term trend (whether it increases or decreases) is a robust conclusion from our numerical study.

Our simulations strongly suggest the existence of a saturation in the disc-driven eccentricity growth, but do not pinpoint the exact value of $e_{\rm crit}$. In the next section we discuss the physical reasons for this limit and analytically predict the value of $e_{\rm crit}$.

4 EXPLANATION OF THE SATURATION

The *growth* of the eccentricity, from initial values e_0 below a critical eccentricity $e_{\rm crit}$, and the *decline* of e from initial values $e_0 > e_{\rm crit}$ call

for a simple physical interpretation. The increase of the eccentricity caused by the interaction of the binary with an external disc is a known fact for very unequal binaries where the non-axisymmetric potential perturbations are small (as in the case of planetary migration, see e.g. Goldreich & Tremaine 1980; Goldreich & Sari 2003; Armitage & Natarajan 2005).

Goldreich & Tremaine (1980) have shown that in the high mass-ratio limit the binary–disc transfer of angular momentum occurs secularly through torques excited in the disc by the binary at discrete Lindblad and corotation resonances. Damping and/or growth of e thus depends on the relative importance of these opposing torques (and hence on how fluid elements are distributed in the disc). Principal Lindblad resonances are known to be responsible for opening a gap in the disc. As a consequence of disc clearance, corotation and inner Lindblad resonances are reduced in power. This consideration led Goldreich & Sari (2003) to show that only the outer Lindblad resonances, remaining after gap opening, cause the increase of the eccentricity for initially low-eccentric binaries.

For the comparable mass limit studied in this paper ($q = 1/3$) we have a simpler explanation. An initially small e increases because of the larger deceleration experienced by the secondary BH near apoapsis with respect to periapsis (see e.g. Lin & Papaloizou 1979; Artymowicz et al. 1991). The longer time spent when nearing apoapsis and the larger overdensity excited in the disc by the hole's gravitational pull due to its immediate proximity are both conducive to a net deceleration of the hole that causes the increase of the binary eccentricity. This increase continues as long as the secondary BH has a larger angular velocity at its apoapsis $\omega_{2,\mathrm{apo}}$ than the fluid elements in the disc ω_{disc}. When this reverses, the density wake excited by the BH moves ahead imparting to the hole, near apoapsis, a net tangential acceleration that tends to increase the angular momentum content of the binary, decreasing e. This argument is valid if the disc and the binary angular momenta are aligned. If they are anti-aligned (i.e. for a retrograde disc) the interaction between the BHs and the gas increases the eccentricity up to $e \approx 1$ (Nixon et al. 2011), resulting in a fast coalescence of the binary. We limit our investigation to discs corotating with the binary, as expected if they form together during a gas-rich galaxy merger (Mayer et al. 2007; Dotti et al. 2009). In this case the torques on the secondary will be minimal if $\omega_{\mathrm{disc}} = \omega_{2,\mathrm{apo}}$. Approximating the binary as a purely Keplerian system and the gaseous disc to be in Keplerian motion around a mass $M_1 + M_2$ located at the system COM, it is easy to derive

$$\omega_{2,\mathrm{apo}}^2 = \frac{GM_1(1+q)}{(1+e)^2 a^3}\left[\frac{2}{(1+e)} - 1\right] \tag{1}$$

$$\omega_{\mathrm{disc}}^2 = \frac{G(M_1+M_2)}{R_{\mathrm{T}}^3}, \tag{2}$$

where we defined R_{T} to be the distance of the strongest torque on the binary as measured from COM. Equating $\omega_{2,\mathrm{apo}}^2 = {\omega_{\mathrm{disc}}}^2$ yields

$$\frac{1}{R_{\mathrm{T}}^3} = \frac{1}{(1+e)^2 a^3}\left[\frac{2}{(1+e)} - 1\right], \tag{3}$$

which can be rearranged as

$$\delta^3 = \frac{(1+e)^3}{(1-e)}, \tag{4}$$

with $\delta = R_{\mathrm{T}}/a$. Equation (4) implies the existence of a limiting eccentricity e_{crit} that we can infer via numerical inversion of equation (4). The expression

$$e_{\mathrm{crit}} = 0.66\sqrt{\ln(\delta - 0.65)} + 0.19 \tag{5}$$

provides an analytical fit to the result within a 2 per cent accuracy in the range $1.8 < \delta < 4.5$, relevant to our study assuming that, in a first approximation, δ can be set equal to the inner edge of the disc, R_{gap}. Note that in this derivation, *for a fixed* δ, e_{crit} is independent of the binary mass ratio. To compare the predictions of this toy model with the simulations, we need to define the inner edge of the disc. This is somewhat tricky since the disc profile is not a step function at a certain R/a. In our initial simulation the clean region within the gap has a size of $R_{\mathrm{gap}} \approx 2a$. At larger distances the disc density increases reaching a maximum around $R/a \approx 2.5$. For $2 < \delta < 2.5$ we get $0.55 < e_{\mathrm{crit}} < 0.69$ which is within the range obtained from the numerical simulations described in Section 3. Note that equation (5) depends on the specific value of δ, i.e. on how close inflows of gas can get to the binary. Even though δ can in principle be measured from our simulations, its value would also be affected by the lack of physical outer-boundary conditions. Instead, δ is usually determined equating the viscous torque in the accretion disc with the positive torque exerted by the binary (see e.g. equation 15 in Artymowicz & Lubow 1994). Artymowicz & Lubow (1994) found that the size of the gap depends on e. For $e \approx 0.6$, $q = 0.3$, disc aspect ratio $H/R = 0.03$ and a viscous parameter $\alpha = 0.1$, they predict $R_{\mathrm{gap}} \approx 2.9a$, corresponding to a 5:1 commensurability resonance. Using this value for δ we would obtain a larger value of $e_{\mathrm{crit}} \approx 0.77$. Note that the interaction between the binary and the disc becomes less efficient as the disc expands, whereas the gravitational pull of the tenuous gas on to the secondary at periapsis increases. So even in a system where the influence of the gas inside the cavity is completely negligible, it is not clear if the binary could reach such a high e_{crit} on a relevant time-scale. Note that a retrograde disc would not expand, since the interaction with the binary decreases its angular momentum. In this case the eccentricity growth remains efficient up to $e \approx 1$ (Nixon et al. 2011).

A direct comparison between our results and the prediction of Artymowicz & Lubow (1994) is not straightforward. Although our self-gravitating disc is able to redistribute angular momentum efficiently, its total amount has to be conserved. Thus, discs hosting very eccentric binaries ($e = 0.6, 0.8$) keep on expanding after a short impulsive interaction with the binary (as discussed in Section 3). The interaction between the disc and the binary is extremely inefficient when $R_{\mathrm{gap}} \gtrsim 4a$ (see the two top panels in Fig. 2). Therefore, although a larger R_{gap}, in first approximation, implies a larger δ implying a larger e_{crit}, it also results in longer time-scales for the eccentricity evolution.

The feeding of a BH binary forming in a gas-rich galaxy merger can be a very dynamic process, and the interaction with a single circumbinary disc could be too idealized a picture. Larger scale simulations show episodic gas inflows due to the dynamical evolution of the nucleus of the remnant (see e.g. Escala 2006; Hopkins & Quataert 2010). In this scenario the binary can still interact with a disc and excavate a gap, but the size of it would be time-dependent (as in the simulations presented here) and would also depend on the angular momentum distribution of the inflowing streams, resulting in a range of e_{crit}.

4.1 Testing the emerging picture

Equation (5) shows that e_{crit} depends on the location of the strongest torque δ and thus, in first approximation, on the size of the gap R_{gap}. In order to cross-check our results, we performed two additional simulations of the $e_0 = 0.8$ case, in which $a(1+e)$ was kept fixed, reducing the semimajor axis by a factor of 1/1.8, thus increasing the *relative* gap size R_{gap} by 80 per cent. These runs simulate a

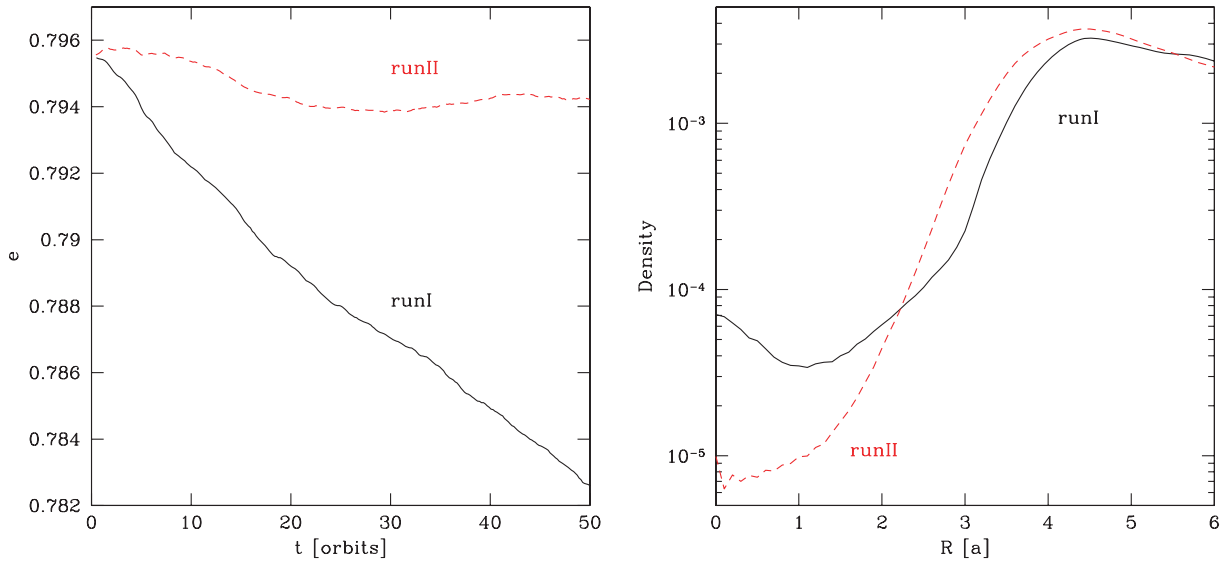

Figure 3. Additional high-eccentricity runs where the initial semimajor axis is reduced by a factor of 1.8, compared to the default runs. These short runs are used to test the emerging picture of a limiting eccentricity depending on the amount of streams present in the cavity. The difference between the two runs is the thermodynamical treatment of the gas inside the cavity. For runI this is identical to the default runs, whereas in runII we suppress gaseous inflows into the gap. Left-hand panel: eccentricity versus time, for $e_0 = 0.8$. Solid line refers to runI, while dashed line to runII. Right-hand panel: azimuthally averaged disc surface density as a function of $R[a]$ in arbitrary units. Surface density is averaged over the orbits 20–30. Solid line refers to runI, dashed line to runII (see text for description).

situation where the infalling material stays at a large distance from the eccentric binary and does not reach $R_{\rm gap} \approx 2.5a$, typical for the low-eccentricity cases presented above.

The analysis performed in the previous section only accounts for the pull of the disc when the secondary is at apoapsis, neglecting torques exerted by the infalling material forming mini-accretion discs around the two BHs. For low e_0, this approximation works well, because the separation of the two BHs is always much larger than the size of the inner mini-discs. However, in the high e_0, small a case tested here, the secondary BH, at each periapsis passage, experiences a significant drag on to the inflowing mass accumulating around the primary. Such drag causes the circularization of the orbit. Therefore, the secular evolution of the binary is determined by two factors: (i) the distance of the gap from the secondary BH at apoapsis and (ii) the amount of inflowing gas through the gap on to the primary BH.

In order to separate the two effects, we set two simulations with identical initial conditions as described above. In runI, we keep exactly the thermodynamics employed in our fiducial runs that allow a stable accretion mini-disc to form around the primary hole; in runII the gas inside the gap evolves with the β-cooling enabled just as in the rest of the disc, and can be heated by adiabatic compression. This suppresses the gaseous inflows into the cavity and prevents the gas from forming a significant circumprimary disc. As shown in the left-hand panel of Fig. 3, runI experiences a substantial steady decline in e, whereas in runII, after a slight initial reduction, the eccentricity stays more or less constant. Such a result confirms our understanding of the dynamics of the system. In runI the secondary encounters the high-density region formed around the primary at each periapsis passage and is slightly decelerated on to a more circular orbit. In runII, after a short initial relaxation phase, there is not enough gas in the centre to cause further circularization (compare the two central densities in the right-hand panel of Fig. 3); on the other hand, the gap is large enough for the disc–binary interaction to be weak and, therefore, the eccentricity growth to be very inefficient. Note also that for a wider binary the same effect holds, however only if the secondary passes through the mini-disc of the primary, the size of which is independent of a. That is why, in comparison to the default runs in Section 3, the effect is visible more clearly here in the case of the narrower binary. Thus, the predicted limiting eccentricity $e_{\rm crit} \approx 0.88$ expected for $\delta = 3.5$ (approximately the size of the gap in these close-separation simulations) cannot be achieved.

Although the torques exerted by the inside-cavity material when the binary eccentricity is high add complexity to the emerging picture, this strengthens the result of a limiting eccentricity in the range $0.6 < e < 0.8$ for the BH binary–disc configurations examined in this paper.

5 OBSERVATIONAL CONSEQUENCES

In this section we focus on the impacts that our findings might have on the long-standing search for close BH binary systems in the Universe. First, we investigate possible periodicities residing in the accretion flows on to the two BHs enhancing our ability to identify such elusive sources. Then, we study the influence of a high limiting eccentricity (attained during migration) on future GW observations with *LISA*.

5.1 Periodically modulated accretion flows

Fig. 4 shows the evolution of the accretion rate $\dot{M}_1$ and $\dot{M}_2$ on to each hole, for the four runs with $e_0 = 0.2, 0.4, 0.6, 0.8$. In order to interpret our results we consider the binary to have a total mass $M = 3.5 \times 10^6\,{\rm M}_\odot$, typical for expected *LISA* detections, and an initial semimajor axis $a_0 = 0.038\,{\rm pc}$. Under this assumption, for a radiative efficiency of 0.1, the Eddington limit would correspond to accretion rates $\dot{M}_{1,{\rm E}} = 0.06\,{\rm M}_\odot\,{\rm yr}^{-1}$ and $\dot{M}_{2,{\rm E}} = 0.02\,{\rm M}_\odot\,{\rm yr}^{-1}$. Fig. 4 shows that this limit is fulfilled for the two high-eccentricity runs only, whereas for the low-e runs the BHs accrete at super Eddington rates. This is possible since the numerics do not include

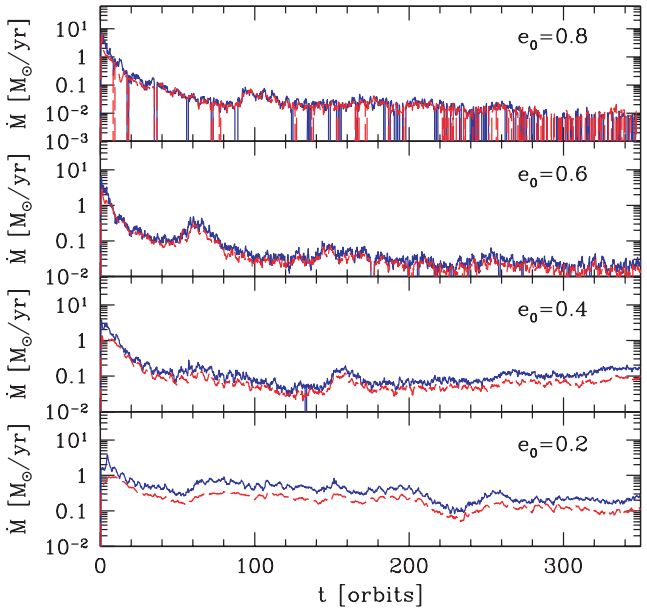

Figure 4. Mass accretion rates on to the BHs, for the runs with $e_0 = 0.2$, 0.4, 0.6, 0.8 (bottom to top). Dashed (red) line refers to the primary BH, solid (blue) line to the lighter secondary hole.

any radiative feedback. The accretion rates drop significantly in the runs with initially higher eccentricity, owing to the expansion of the gap size with time (as discussed in Section 3).

Fig. 5 shows the power spectra of the accretion rates $\dot{M}$ on to the two BHs. The frequency f (on the x-axis) is in units of the binary orbital frequency f_0, and the power spectral density in arbitrary units. A clear periodicity emerges at the orbital frequency f_0, indicating a modulation of the inflow rate, induced by the orbital motion (Artymowicz & Lubow 1996; Hayasaki, Mineshige & Ho 2008). Note that smearing of the peaks at $\sim f_0$, in Fig. 5, for $e_0 = 0.2$ and 0.4, is due to the a few per cent shrinking of the semimajor axis, and therefore also of the orbital period, during the evolution. As the binary eccentricity increases, the second and third harmonics of the orbital frequency increase in power and become visible. In the inlay of each panel the power spectrum associated to the total mass transfer rate on to the binary is plotted in the frequency range $0.1f_0 < f < 1.0f_0$ to illustrate the presence of other characteristic features at (i) the frequency associated to the rotation of the fluid in the dense part of the disc: $f_{\rm disc}/f_0 = (a_0/r_{\rm disc})^{3/2}$ and (ii) the beat frequency, i.e. the difference between the binary and the disc rotation frequencies: $f_{\rm beat}/f_0 = 1 - (a_0/r_{\rm disc})^{3/2}$. Here $r_{\rm disc}$ denotes the radial distance where the disc surface density has its maximum. Since the disc has a broad density profile, we consider the two values r_- and r_+ defined by the full width at half-maximum of the density

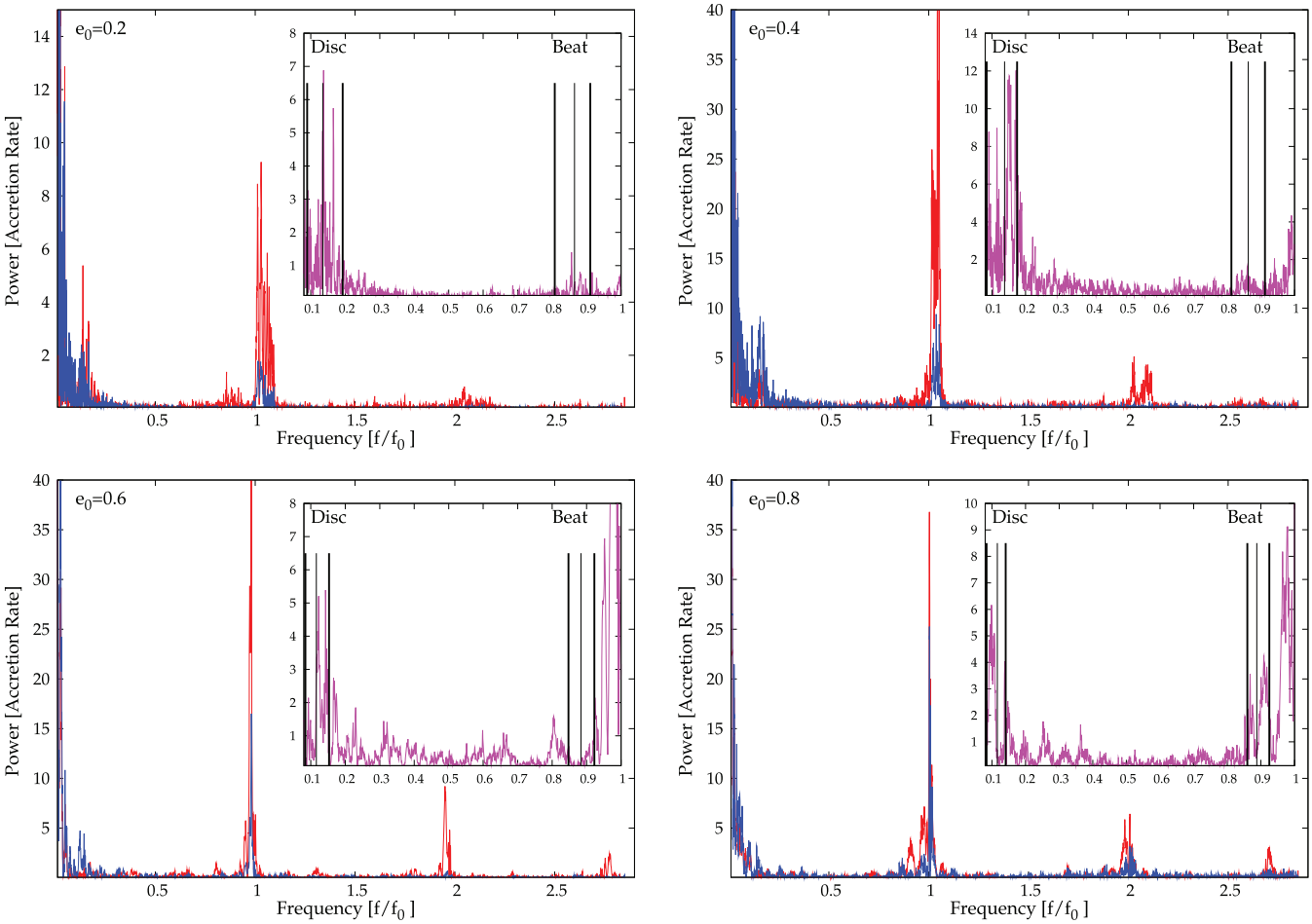

Figure 5. Power spectrum of the accretion rate (in arbitrary units^2) on to the primary (blue) and secondary (red) BHs. Frequencies are in units of the initial binary orbital frequency f_0. The inlays show zoom-ins of the power spectra, in the frequency range 0.1–1f_0 computed summing the accretion rate from the two BHs (pink). The expected intervals for the disc and the beat frequencies are marked by the thick vertical black lines, as labelled in the figure.

and use those to estimate the expected disc and beat frequency intervals (enclosed by the two pairs of thick black lines in the inset of Fig. 5). As expected, we observe broad features consistent with the predicted frequency ranges. Signatures of the disc are always visible in these plots, with a complex line structure mirroring the overdensities in its spiral arms. The beat is very distinct in the $e_0 = 0.8$ run, while it is marginally visible in the other runs. We further note that the significance of the peak[2] in the power spectrum, at the binary orbital frequency f_0, is weaker for low-eccentric binaries ($e_0 = 0.2$) than for binaries with higher eccentricities. This agrees with previous works (cf. Cuadra et al. 2009) that show a mild periodicity in the accretion rate in the case of quasi-circular binaries. Thus, a periodic signal is expected to be a distinctive signature of eccentric massive BH binaries.

The presence of periodicities in the accretion flows opens interesting prospects for monitoring subparsec BH eccentric binaries in circumbinary discs. Our fiducial system has $M = 3.5 \times 10^6\,\mathrm{M}_\odot$ and an initial semimajor axis $a_0 = 0.038\,\mathrm{pc}$ corresponding to an orbital period of 348 yr, exceeding a human lifetime. Since the binary fingerprints in the accretion rates are related to the dynamical time, we can extrapolate our results to smaller periods as long as the disc and the binary are dynamically coupled (see the next section). For a binary with $M = 3.5 \times 10^6\,\mathrm{M}_\odot$ and $q = 1/3$, binary–disc coupling may survive down to much shorter periods of $\sim$1 month, making the observation of such periodicities astrophysically feasible. The interval of modulation $\Delta(\dot{M})$ from our runs is at the level of $\Delta(\dot{M}) \in [10, 50]$ per cent for $e_0 = 0.2$, $\in [40, 100]$ per cent for 0.4, $\in [40, 90]$ per cent for 0.6 and $\in [10, 50]$ per cent for 0.8. Assuming a luminosity proportional to the time-dependent accretion rate, a periodic monitoring of such sources will allow us to construct the light curve for several years. An amplitude modulation of up to 100 per cent over 10–100 cycles will thus be easily identifiable.

5.2 Residual eccentricity in GW observations

The existence of a limiting eccentricity that is maintained during the coupled evolution of the disc–binary system has important consequences for the detection of the binary as GW source in the latest stage of its evolution, i.e. during the last year of GW inspiral towards coalescence. Since the systems in our simulations are far from coalescence (in our fiducial rescaling $a = 0.038\,\mathrm{pc}$, corresponding to $\sim 10^5$ Schwarzschild radii of the primary hole), in the following we will extrapolate our findings to much smaller scales (order of $\sim 10^3$ Schwarzschild radii) making use of the standard optically thick, geometrically thin α-disc recipe (Shakura & Sunyaev 1973).

In the standard picture of BH migration, the BHs reach closer separations under the action of viscous torques exerted by the circumbinary disc. This holds true as long as the migration time-scale t_m is shorter than the binary GW decay time-scale t_GW. Since the former scales as $\propto a^{7/8}$ or $a^{35/16}$ for gas and radiation pressure supported discs (Haiman et al. 2009), while the latter as $\propto a^4$, there will eventually be a critical separation a_dec below which GW emission takes over and the binary decouples from the disc. After decoupling, binary–disc mutual torques are ineffective and the binary evolution is driven by GWs only. GWs tend to circularize the binary, but if decoupling occurs at small a, there might not be enough room for complete orbit circularization before entering the *LISA* frequency domain. Even a residual eccentricity as small as $e \sim 10^{-4}$ may be easily detectable (Cornish & Key 2010), and it has to be accounted for, for a trustworthy parameter estimation of the GW source (Porter & Sesana 2010).

To estimate the residual eccentricity in the *LISA* band e_LISA we need four ingredients:

(i) the binary eccentricity at decoupling, e_dec;
(ii) the binary semimajor axis at decoupling, a_dec;
(iii) a model for the GW decay after decoupling and
(iv) an estimation of f_LISA at which e_LISA has to be computed.

Being interested in *LISA* BH binaries, we consider systems characterized by $10^5\,\mathrm{M}_\odot < M_1 < 10^7\,\mathrm{M}_\odot$ and $0.01 < q < 1$. Item (i) is directly extracted from the simulations and the analytical argument presented in this paper. We assume that, at decoupling, the binary has the limiting eccentricity e_crit given by equation (2).

Because of its small extent, the circumbinary disc assumed in our simulations is unable to transfer the binary angular momentum outwards efficiently for a prolonged time-scale. It is therefore unsuitable for estimating a disc-driven binary decay rate to be compared to the GW angular momentum loss. A viable shortcut to compute a_dec [item (ii)] is to link our disc to a standard thin accretion disc and to estimate the gas-driven migration time-scale in that approximation. When scaled to physical units, our binary has $a_0 = 0.038\,\mathrm{pc}$. At such a separation, the circumbinary disc can be described as a steady-state, geometrically thin, optically thick Shakura–Sunyaev α-disc (Haiman et al. 2009). Accordingly, the disc has a mass

$$M_\mathrm{d} = 1.26 \times 10^3\,\mathrm{M}_\odot\,\alpha_{0.3}^{-4/5}\left(\frac{\dot{m}}{\epsilon_{0.1}}\right)^{7/10} M_7^{11/5}\left(R_\mathrm{out}^{5/4} - R_\mathrm{in}^{5/4}\right), \quad (6)$$

where $\alpha_{0.3}$ is viscosity parameter normalized to 0.3, $\dot{m} = \dot{M}/\dot{M}_\mathrm{E}$ is the accretion rate (in units of the Eddington rate), $\epsilon_{0.1}$ is the radiative efficiency normalized to 0.1 and M_7 is the total mass of the binary in units of $10^7\,\mathrm{M}_\odot$; the two limiting radii of the disc, R_in and R_out, are expressed in units of $10^3 R_\mathrm{Sch}$ (with $R_\mathrm{Sch} = 2GM/c^2$) and correspond to $R_\mathrm{in} = 2a_0$ and $R_\mathrm{out} = 10a_0$, respectively. With this choice we infer a total disc mass $M_\mathrm{d} \sim 0.25M$ which is comparable to our relaxed disc. In such a disc the time-scale for migration of the secondary BH on to the primary is given by (equation 26a of Haiman et al. 2009)[3]

$$t_\mathrm{m} = 1.5 \times 10^5\,\mathrm{yr}\,M_7^{5/8} q_\mathrm{s}^{3/8} \tilde{a}_3^{35/16}, \quad (7)$$

where now $\tilde{a}_3$ is the binary semimajor axis in units of $10^3 R_\mathrm{Sch}$ and $q_\mathrm{s} = 4q/(1+q^2)$ is the symmetric binary mass ratio. This time-scale has to be compared with the GW decay time-scale for an eccentric binary which, in the quadrupole approximation, is given by (Peters & Mathews 1963)

$$t_\mathrm{GW} = a\frac{\mathrm{d}t}{\mathrm{d}a} = 7.84 \times 10^6\,\mathrm{yr}\,M_7 q_\mathrm{s}^{-1} \tilde{a}_3^4 F(e)^{-1}, \quad (8)$$

[2] We utilize the normalized Lomb–Scargle periodogram here, wherein the significance of each peak is directly given by the false-alarm probability (FAP) (Scargle 1982). Since the number of independent frequencies is the same for all four runs, the FAP scales identically for all runs, thus the relative height translates into significance. For our runs, a peak needs to exceed a height of 12 in order to have an FAP of 0.01.

[3] We note that equation 26a of Haiman et al. (2009) is an extrapolation of radiation supported α-discs using the Syer & Clarke (1995) solution to the type II migration problem. Such a solution is, however, strictly applicable to discs with surface density which is a decreasing function of the radius, and it therefore breaks down in the radiation supported α-disc case. To check that our results do not depend on the specific disc assumptions, we also considered a radiation+gas supported β-disc (for which the Syer & Clarke solution applies, see Haiman et al. 2009 for details) and found no significant difference in the residual eccentricity, relevant to GW observations.

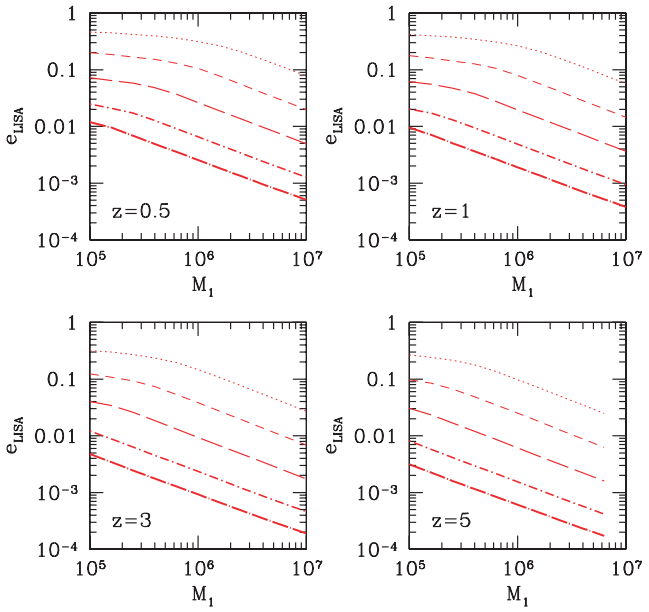

Figure 6. Residual eccentricity $e_{\rm LISA}$ as a function of M_1, for different mass ratios. Each panel refers to BH binaries at different redshifts as labelled in the figure. In each panel, from bottom to top, curves are for $\log q = 0, -0.5, -1, -1.5, -2$.

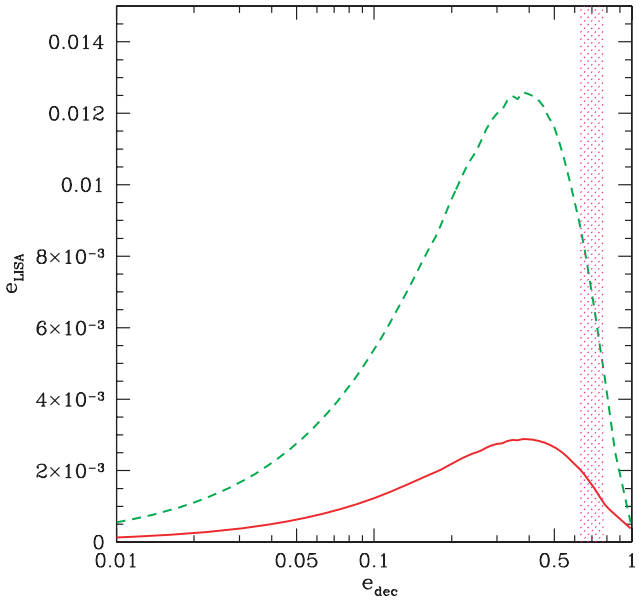

Figure 7. Residual eccentricity $e_{\rm LISA}$ as a function of $e_{\rm dec}$. Red solid curve refers to $q = 1/3$, green dashed curve to $q = 0.1$. In the figure the mass of the primary BH is $M_1 = 2.6 \times 10^6\,{\rm M}_\odot$ and the redshift of the binary is $z = 1$. The shaded vertical stripe brackets the limiting eccentricity interval found in our simulations.

where

$$F(e) = (1-e^2)^{-7/2}\left(1 + \frac{73}{24}e^2 + \frac{37}{96}e^4\right). \quad (9)$$

The disc–binary decoupling occurs when $t_{\rm GW} = t_{\rm m}$, and this happens somewhere in the range of binary separations $a_{\rm dec} \sim 10^2$–$10^3 R_{\rm Sch}$, depending on the binary mass and mass ratio. From that point on, the dynamics of the binary is driven by GW emission only.

To address point (iii), we integrate the post-Newtonian equation for eccentric binaries given by Junker & Schaefer (1992), following the eccentricity evolution down to the last stable orbit. *LISA* will be sensitive to GWs in the frequency range 10^{-4}–0.1 Hz and, in general, it will be able to monitor the final year of the binary evolution with high signal-to-noise ratio. We therefore set [item (iv)] $f_{\rm LISA} = \max[10^{-4}\,{\rm Hz}, f(1\,{\rm yr})]$, where $f(1\,{\rm yr})$ is the GW frequency observed 1 yr before the final coalescence. Note that the observed GW frequency is related to the rest-frame emitted frequency $f_{\rm r}$ as $f = f_{\rm r}/(1+z)$. This means that $e_{\rm LISA}$, defined as the eccentricity of the BH binary at the time of entrance in the *LISA* band, depends on the source redshift. The 10^{-4} Hz cut-off in observed frequency corresponds to higher emitted frequencies as z increases; binaries at higher z will be caught closer to coalescence and will therefore show a lower residual eccentricity.

The predicted values of $e_{\rm LISA}$, as a function of M_1 for different q and z, are shown in Fig. 6. Not surprisingly, the residual eccentricity is larger for lighter binaries (i.e. for lighter M_1) and smaller mass ratios q. This is simply a consequence of the scaling with M and $q_{\rm s}$ of the frequency at decoupling, $f_{\rm dec}$, and can be easily understood analytically as follows. By coupling the orbital decay rate to the eccentricity decay rate in the quadrupole approximation (sufficient for a scaling argument, Peters & Mathews 1963), we get

$$\frac{f_{\rm r}}{f_{\rm o}} = \left\{\frac{1-e_{\rm o}^2}{1-e^2}\left(\frac{e}{e_{\rm o}}\right)^{12/19}\left[\frac{1+\frac{121}{304}e^2}{1+\frac{121}{304}e_{\rm o}^2}\right]^{870/2299}\right\}^{-3/2}, \quad (10)$$

where $f_{\rm r} = 2f_{\rm K}$ is the frequency of the fundamental GW harmonic (in the rest frame of the source) inferred from Kepler's law $a^3 = GM/(2\pi f_{\rm K})^2$. Equation (10) allows us to compute e at any given frequency $f_{\rm r}$, once $e_{\rm o}$ and $f_{\rm o}$ are provided. In our case $e_{\rm o} = e_{\rm dec} \sim 0.6$ and $f_{\rm o} = f_{\rm dec}(a_{\rm dec})$. If we set the value $f_{\rm LISA} = 10^{-4}$ Hz as final frequency, equation (10), in the limit of small final e, gives

$$e_{\rm LISA} \propto f_{\rm dec}^{19/18}. \quad (11)$$

The identity $t_{\rm m} = t_{\rm GW}$ requires $a_{\rm dec} \propto M^{23/29} q_{\rm s}^{22/29}$. Coupling this result to Kepler's law (i.e. $a^3 \propto M f_{\rm r}^{-2}$), we get $f_{\rm dec} \propto M^{-20/29} q_{\rm s}^{-33/29}$. Finally, using equation (11) we obtain

$$e_{\rm LISA} \propto M^{-0.73} q_{\rm s}^{-1.2}, \quad (12)$$

which is basically the M and q dependence observed in Fig. 6. Fig. 7 shows how this result depends on the binary eccentricity at decoupling. We see two interesting things: first, there is a maximum $e_{\rm LISA}$ at $e_{\rm dec} \approx 0.4$ (i.e. $e_{\rm LISA}$ is not a monotonic function of $e_{\rm dec}$)and, secondly, as long as $0.1 < e_{\rm dec} < 0.7$, $e_{\rm LISA}$ changes only within a factor of $\approx$2. This is a consequence of the $t_{\rm GW}$ dependence on e. The higher the e, the faster the GW-driven evolution, and the larger the $a_{\rm dec}$. Even though $e_{\rm dec}$ is larger, the binary has much more time to circularize before entering the *LISA* band, showing a smaller residual eccentricity $e_{\rm LISA}$. We note that the exact value of $e_{\rm LISA}$ depends on the disc properties. It is, however, interesting that a small $e_{\rm LISA}$ can be associated both to a fairly circular $e_{\rm dec} \approx 0.05$ binary and to a binary with $e_{\rm dec} > 0.95$.

These results obviously depend on the assumed disc parameters. Both a lower $\dot{m}$ and a lower α would increase $t_{\rm m}$, resulting in a larger $a_{\rm dec}$ and, in turn, in a smaller $e_{\rm LISA}$. On the other hand, if the BHs have large spins, the radiative efficiency ϵ may be up to a factor of 3 larger, acting in the opposite direction. It is however worth to keep in mind that $t_{\rm GW} \propto a^4$. A change of a factor of 10 on $t_{\rm m}$ will therefore result in a change of about $\sim 1.8 a_{\rm dec}$, eventually influencing $e_{\rm LISA}$ only by a factor of 2. We can therefore

consider our results robust and only mildly dependent on the details of the disc.

6 CONCLUSIONS

In this paper, we explored the dynamics of subparsec BH binaries interacting with a circumbinary gaseous disc after they have excavated a gap in the surface density distribution. We ran a sequence of numerical models that differ only in the initial binary eccentricity e_0. Our aim was to study the evolution of the eccentricity in order to answer the following question: does the eccentricity (which is known to increase in initially circular binaries) continue to grow up to $e \rightarrow 1$ so that BH binaries in such discs reach the GW domain on a nearly zero angular momentum orbit, or does e saturate, and if so, at which value?

The key finding is that e converges to a limiting value $e_{\rm crit}$. Binaries that start with low eccentricities ($e_0 < e_{\rm crit}$) increase e up to $e_{\rm crit}$, whereas binaries that start with high eccentricities ($e_0 > e_{\rm crit}$) display the opposite behaviour, i.e. their eccentricity declines with time approaching $e_{\rm crit}$. Saturation rises due to the opposing action of the gravitational drag experienced by the lighter, secondary BH in its motion near apoapsis. For low-eccentricity orbits, the secondary BH excites a density wake which lags behind the BH at apoapsis, causing its deceleration (and so a rise of e). The opposite occurs for a highly eccentric orbit: the secondary moves more slowly than the disc (i.e. its angular frequency is smaller than the angular frequency of the adjacent fluid elements) and the density wake moves ahead of the BH path, causing a net acceleration. Using this simple analytical argument, the limiting eccentricity is independent of the binary mass ratio, but is a function of the location δ of the inner rim of the disc from the system COM. For the range of values $2 < \delta < 2.5$, this argument predicts $0.55 < e_{\rm crit} < 0.79$, consistent with our numerical findings. The larger the gap size, the higher the $e_{\rm crit}$ and the longer the time-scale on which this limit is attained . The expectation is that BH binaries, immersed in circumbinary discs, maintain a large eccentricity throughout the migration process. Although in this study we have focused on BH binaries, the evolution of protostellar binaries occurs in a similar geometry (e.g. Artymowicz & Lubow 1994; Bate 1997) and shares much of the same physics. Thus, our results are likely relevant for the interpretation of the observed distribution of binary star eccentricities (e.g. Pourbaix et al. 2004).

The existence of a relatively large limiting eccentricity in a BH binary that emerges from the migration phase has two important observational consequences. There is the possibility of triggering periodic inflows of gas on to the two BHs. This would enhance the possibility of an electromagnetic identification of a subparsec BH binary. Here we showed that periodicities occur on the dynamical time related to the Keplerian motion of the binary (depending on the binary parameters, from months to hundreds of years) and of the inner rim of the circumbinary disc, together with the beat frequency between the two. These features should be discernible in the power spectra of active nuclei, and this issue will be explored in detail in a forthcoming paper. Also, a feasible GW signature of a BH binary that evolved through disc migration is a detectable residual eccentricity at the time of entrance in the *LISA* band. In the case of our set-up this residual e would amount to $e_{\rm LISA} \sim 2 \times 10^{-3}$ for a coalescing source at $z = 1$, but can be as high as $e_{\rm LISA} > 0.1$ for a lower mass, lower q binary (with $M \sim 10^5\,{\rm M}_\odot$ and $q < 0.1$) at the same redshift. Thus, this study has an impact both on searches of periodicities in the light curves of active BHs and on GW data stream analysis.

ACKNOWLEDGMENTS

We thank the anonymous referee for suggestions that greatly improve the presentation of our results. We thank Pau Amaro Seoane, Luciano Rezzolla and Julian Krolik for useful discussions. CR wishes to thank Nico Budewitz for support in all HPC matters. The computations were performed in the Damiana cluster of the AEI. JC acknowledges support from FONDAP Center for Astrophysics (15010003), FONDECYT (Iniciación 11100240) and VRI-PUC (Inicio 16/2010).

REFERENCES

Amaro-Seoane P., Eichhorn C., Porter E. K., Spurzem R., 2010, MNRAS, 401, 2268
Armitage P. J., Natarajan P., 2002, ApJ, 567, L9
Armitage P. J., Natarajan P., 2005, ApJ, 634, 921
Artymowicz P., Lubow S. H., 1994, ApJ, 421, 651
Artymowicz P., Lubow S. H., 1996, ApJ, 467, L77
Artymowicz P., Clarke C. J., Lubow S. H., Pringle J. E., 1991, ApJ, 370, L35
Bate M. R., 1997, MNRAS, 285, 16
Bate M. R., Bonnell I. A., Price N. M., 1995, MNRAS, 277, 362
Begelman M. C., Blandford R. D., Rees M. J., 1980, Nat, 287, 307
Berentzen I., Preto M., Berczik P., Merritt D., Spurzem R., 2009, ApJ, 695, 455
Colpi M., Dotti M., 2009, preprint (arXiv:0906.4339)
Cornish N. J., Key J. S., 2010, Phys. Rev. D, 82, 044028
Cuadra J., Nayakshin S., Springel V., Di Matteo T., 2006, MNRAS, 366, 358
Cuadra J., Armitage P. J., Alexander R. D., Begelman M. C., 2009, MNRAS, 393, 1423
Dotti M., Colpi M., Haardt F., Mayer L., 2007, MNRAS, 379, 956
Dotti M., Ruszkowski M., Paredi L., Colpi M., Volonteri M., Haardt F., 2009, MNRAS, 396, 1640
Escala A., 2006, ApJ, 648, L13
Escala A., Larson R. B., Coppi P. S., Mardones D., 2005, ApJ, 630, 152
Goldreich P., Sari R., 2003, ApJ, 585, 1024
Goldreich P., Tremaine S., 1980, ApJ, 241, 425
Gould A., Rix H., 2000, ApJ, 532, L29
Haiman Z., Kocsis B., Menou K., 2009, ApJ, 700, 1952
Hayasaki K., Mineshige S., Ho L. C., 2008, ApJ, 682, 1134
Hopkins P. F., Quataert E., 2010, MNRAS, 407, 1529
Ivanov P. B., Papaloizou J. C. B., Polnarev A. G., 1999, MNRAS, 307, 79
Junker W., Schaefer G., 1992, MNRAS, 254, 146
Lin D. N. C., Papaloizou J., 1979, MNRAS, 186, 799
Lodato G., Nayakshin S., King A. R., Pringle J. E., 2009, MNRAS, 398, 1392
Mayer L., Kazantzidis S., Madau P., Colpi M., Quinn T., Wadsley J., 2007, Sci, 316, 1874
Merritt D., Milosavljević M., 2005, Living Rev. Relativ., 8, 8
Nixon C. J., Cossins P. J., King A. R., Pringle J. E., 2011, MNRAS, 412, 1591
Papaloizou J., Pringle J. E., 1977, MNRAS, 181, 441
Peters P. C., Mathews J., 1963, Phys. Rev., 131, 435
Porter E. K., Sesana A., 2010, preprint (arXiv:1005.5296)
Pourbaix D. et al., 2004, A&A, 424, 727
Price D. J., 2007, Publ. Astron. Soc. Australia, 24, 159
Rice W. K. M., Lodato G., Armitage P. J., 2005, MNRAS, 364, L56
Scargle J. D., 1982, ApJ, 263, 835
Sesana A., 2010, ApJ, 719, 851
Shakura N. I., Sunyaev R. A., 1973, A&A, 24, 337
Springel V., 2005, MNRAS, 364, 1105
Syer D., Clarke C. J., 1995, MNRAS, 277, 758

This paper has been typeset from a TEX/LATEX file prepared by the author.